

Effect of ultra-low doses, ASIR and MBIR on density and noise levels of MDCT images of dental implant sites

Gerlig Widmann¹ · Reema Al-Shawaf² · Peter Schullian¹ · Ra'ed Al-Sadhan² · Romed Hörmann³ · Asma'a A. Al-Ekrish²

Received: 9 December 2015 / Revised: 28 July 2016 / Accepted: 29 August 2016 / Published online: 21 September 2016
© European Society of Radiology 2016

Abstract

Objectives Differences in noise and density values in MDCT images obtained using ultra-low doses with FBP, ASIR, and MBIR may possibly affect implant site density analysis. The aim of this study was to compare density and noise measurements recorded from dental implant sites using ultra-low doses combined with FBP, ASIR, and MBIR.

Gerlig Widmann and Asma'a A. Al-Ekrish contributed equally to this work.

Electronic supplementary material The online version of this article (doi:10.1007/s00330-016-4588-8) contains supplementary material, which is available to authorized users.

✉ Asma'a A. Al-Ekrish
asma.alekrish@gmail.com; aalekrish@ksu.edu.sa

Gerlig Widmann
gerlig.widmann@i-med.ac.at

Reema Al-Shawaf
reema_alshawaf@yahoo.com

Peter Schullian
peter.schullian@i-med.ac.at

Ra'ed Al-Sadhan
rsadhan@ksu.edu.sa

Romed Hörmann
romed.hoermann@i-med.ac.at

¹ Department of Radiology, Medical University of Innsbruck, Innsbruck, Austria

² Department of Oral Medicine and Diagnostic Sciences, College of Dentistry, King Saud University, P. O. Box 56810, Riyadh 11564, Kingdom of Saudi Arabia

³ Division of Clinical and Functional Anatomy, Medical University of Innsbruck, Innsbruck, Austria

Methods Cadavers were scanned using a standard protocol and four low-dose protocols. Scans were reconstructed using FBP, ASIR-50, ASIR-100, and MBIR, and either a bone or standard reconstruction kernel. Density (mean Hounsfield units [HUs]) of alveolar bone and noise levels (mean standard deviation of HUs) was recorded from all datasets and measurements were compared by paired *t* tests and two-way ANOVA with repeated measures.

Results Significant differences in density and noise were found between the reference dose/FBP protocol and almost all test combinations. Maximum mean differences in HU were 178.35 (bone kernel) and 273.74 (standard kernel), and in noise, were 243.73 (bone kernel) and 153.88 (standard kernel).

Conclusions Decreasing radiation dose increased density and noise regardless of reconstruction technique and kernel. The effect of reconstruction technique on density and noise depends on the reconstruction kernel used.

Key Points

- Ultra-low-dose MDCT protocols allowed more than 90 % reductions in dose.
- Decreasing the dose generally increased density and noise.
- Effect of IRT on density and noise varies with reconstruction kernel.
- Accuracy of low-dose protocols for interpretation of bony anatomy not known.
- Effect of low doses on accuracy of computer-aided design models unknown.

Keywords Algorithms · Dental implants · Image processing, computer-assisted · Multidetector computed tomography · Radiation dosage

Acronyms

ASIR	Adaptive statistical iterative reconstruction
MBIR	Model-based iterative reconstruction
FBP	Filtered backprojection

Introduction

Assessment of bone density from multidetector computed tomography (MDCT) images using Hounsfield units (HUs) is considered an objective, accurate, and stable measurement [1, 2]. In imaging of dental implant sites, positive correlations have been reported between various measures of primary implant stability and bone density measurements recorded from MDCT [3–6] and quantitative CT [7–9]. Furthermore, due to the accuracy in thresholding and segmentation of MDCT data, it has been found to be one of the most accurate modalities in production of 3D models of the jaws [10–13], which is significant when MDCT is used in the production of surgical stents for dental implant surgery.

However, the increasing use of MDCT has been cited as a cause for the increasing collective dose of ionizing radiation to populations [14], and cone beam CT (CBCT) has been advocated as imparting lower radiation doses to patients, and is increasingly becoming more available to oral implantologists. MDCT, though, is still utilized by many practitioners, and the position statement of the American Academy of Oral and Maxillofacial Radiology on selection criteria for the use of radiology in dental implantology recognizes the continued use and need for MDCT in oral implantology, but stresses that dose-sparing protocols should be used whenever possible without adversely affecting diagnostic accuracy [15]. The remarkable progress in MDCT technology has produced devices with more detectors, allowing faster scanning times and low-dose exposures [16, 17], and the reported doses from ultra-low-dose MDCT protocols [18] are lower than those reported for several dentomaxillofacial CBCT devices [19, 20]. Further, the use of various iterative reconstruction techniques (IRTs), such as adaptive statistical iterative reconstruction (ASIR) and model-based iterative reconstruction (MBIR) has shown improvements in MDCT image quality with reduced radiation doses, when compared with the traditionally used filtered backprojection technique (FBP) [18, 21]. However, the resultant images reportedly demonstrate an "oversmoothing" effect [18, 22], of which the effect on density and thresholding must be considered. Also, the HU scale may vary when the MDCT exposure parameters are lowered, especially x-ray beam energy (kVp) [23, 24].

At the time of writing, to our knowledge, there is no information in the published literature regarding the effect of considerable dose reductions in combination with various IRTs on the combined HU and noise levels in dental implant site imaging. The variations within these objective measurements

needs to be investigated to understand how the use of low-dose IRT protocols may affect analysis of bone density of implant sites and computer guided surgery. Therefore, this study aimed to compare the objective density and noise measurements recorded from MDCT images of dental implant sites using ultra-low doses combined with FBP, ASIR and MBIR with those from a standard dose/FBP protocol, and to investigate the effect of dose and reconstruction technique on the measurements.

Materials and methods

Cadaver selection

Two cadaveric heads (one edentulous and one partially dentulous) with intact soft tissues were used in the study. The bodies were donated by people who had given their informed consent for their use for scientific and educational purposes prior to death. The study fulfilled all requirements necessary for studies on human cadavers according to the regulations of the Division of Clinical and Functional Anatomy, Medical University of Innsbruck [25, 26]. All cadavers were preserved using an arterial injection of an alcohol-glycerin solution and immersion in phenolic acid in water for 1 to 3 months [27].

Imaging of the cadavers

The cadaver heads including the mandible were scanned using a 64-multi-slice CT scanner (Discovery CT750 HD, GE Healthcare, Vienna, Austria). The scan range included the entire skull and mandible. Each cadaver was exposed to a high-resolution reference protocol and four low-dose protocols (Table 1). The pitch factor for all protocols was 0.5. There was no movement of the cadavers during and between the five different exposures. In addition to the FBP standard reconstruction all images were reconstructed using the following IRTs: ASIR-50, ASIR-100, and MBIR. Adaptive statistical iterative reconstruction (GE Healthcare) uses information obtained from the FBP algorithm but integrates a comparison of the pixel values with an ideal value to selectively identify and then subtract noise from an image at adaptive blend levels which are freely selectable, typically from 10 % to 100 %. [22] The ASIR reconstructions used in the present study were ASIR-50 (50 % FBP and 50 % ASIR) and ASIR-100 (100 % ASIR). A bone convolution kernel was used in the images of cadaver 1 (except with MBIR for which only a standard convolution kernel was available). A standard reconstruction kernel was used in all the images of cadaver 2. The volume CT dose index ($CTDI_{vol}$) and dose length product (DLP) were obtained from the digital imaging and communication in medicine (DICOM) tags. In

Table 1 List of exposure parameters and reconstruction techniques used to produce the various combinations of MDCT image datasets. Dose length product (DLP) and effective dose include the scan of the entire skull and mandible

Dose protocol	Reconstruction technique	kV	mAs	Pitch	CTDI _{vol} (mGy)	DLP (mGy*cm)	Effective dose (microSv)*	
Reference dose	FBP	120	100	0.5	36.71 ^a	931.3 ^a	4000 ^a	
	ASIR 50				30.48 ^b		3800 ^b	
	ASIR 100							
	MBIR							
Low-dose protocol 1	FBP	100	35	0.5	4.19 ^a	106.22 ^a	500 ^a	
	ASIR 50				3.48 ^b		400 ^b	
	ASIR 100							
	MBIR							
Low-dose protocol 2	FBP	80	40	0.5	2.64 ^a	66.91 ^a	300	
	ASIR 50				2.19 ^b			61.6 ^b
	ASIR 100							
	MBIR							
Low-dose protocol 3	FBP	80	15	0.5	0.99 ^a	25.11 ^a	100	
	ASIR 50				0.82 ^b			23.08 ^b
	ASIR 100							
	MBIR							
Low-dose protocol 4	FBP	80	10	0.5	0.53 ^a	13.38 ^a	100	
	ASIR 50				0.44 ^b			12.29 ^b
	ASIR 100							
	MBIR							

* Calculated by CTEXPO software

^a Cadaver 1

^b Cadaver 2

In addition, effective doses were calculated using CT-Expo V 2.1 (Medical University Hannover, Germany), an MS Excel application for assessing the radiation doses delivered to patients undergoing CT examinations based on the scan parameters of the used scanner type. A protocol summary can be found in Table 1.

Processing and viewing of 3D datasets

Each of the 40 MDCT data sets was converted to DICOM format and uploaded onto a shared Google drive. The DICOM data sets were then imported into a 3D image reformatting software (OnDemand Software, version 1.0, Cybermed Inc., Seoul, South Korea). The images were viewed on a 22" flat panel LCD colour monitor in landscape mode (Dell P2210, Round Rock, TX, USA). Specifications of the monitor were as follows: aspect ratio: 16:10; screen resolution 1680 × 1050 (highest, recommended; calculated pixel size: 0.282 mm); colour resolution: 32 bit; luminance 250 Cd/m²; contrast ratio (static): 1000:1. The window width/level of the MDCT images was set to 3000/650, and the images were viewed and measurements recorded in a dimly lit room.

Sample selection

The maxillary and mandibular edentulous ridges of both the imaged cadavers provided the study sample sites. The sample site inclusion criteria were all edentulous spaces within the jaws of the cadavers, at 5-mm intervals. The exclusion criteria for the edentulous spaces were the following: presence of foreign objects or artificial defects at the residual ridge, and areas of residual ridges where the standardized position of the region of interest (ROI) included non-osseous tissues. Based upon the inclusion and exclusion criteria, 41 sample sites were obtained (25 sites from cadaver 1 and 16 sites from cadaver 2). All the sample sites were in areas of the data sets which were not degraded by artifacts from foreign bodies or dental restorations.

Reformatting of sample sites

One oral and maxillofacial radiologist (A.A.) with 10 years experience in CT image processing and analysis performed the reformatting of all the datasets to obtain transverse cross-sectional images of the sample sites. The 3D module of the OnDemand software was used to produce each cross-section individually. The text overlay information was turned off in

order to mask the mA, and kVp. Since the cadaver heads were not moved between the MDCT examinations, the default position and orientation of the orthogonal sectional planes relative to the jaws were consistent in all the MDCT datasets of each cadaver. Thus, standardization of the site and orientation of the reformatted sample sites was achievable through measured shift and angulation of the orthogonal sectional planes. The contrast and density and zoom level were also standardized amongst all images. Each reformatted site was saved as a bookmark on the master database of the reformatting software (on the hard drive of the computer) such that the examiners can access the reformatted sites using the OnDemand software.

Recording the test measurements

Two independent examiners who were blinded to the exposure parameters and reconstruction protocols recorded the test measurements. The examiners were OMF radiologists with 10 and 5 years experience in MDCT image processing and analysis. The ROI tool of the software was used to select a square area 4×4 mm in size which was positioned at the intersection of the axial and para-sagittal reformatting lines at the sample sites. Tables 2 and 3 show sample sites, with ROIs, obtained with each of the 20 combinations of dose protocols and reconstruction techniques using a bone kernel and standard kernel, respectively. The mean values for the HUs within each ROI were used to analyze density, and the standard deviation within each ROI was used to analyze the noise levels.

The first examiner recorded all the measurements once. For reliability testing, 100 sample sites were selected to be equally distributed amongst the imaging protocols; five samples were randomly selected from each protocol (three sites randomly selected from cadaver 1 and two sites randomly selected from cadaver 2). An online random number generator was used for random selection of sites (<http://stattrek.com/statistics/random-number-generator.aspx>). The first and second examiners recorded the measurements from the 100 sites independently, with at least a 1-week interval between the first and second recordings by the first examiner.

Statistical analysis

The recorded measurements were analyzed with the statistical program: SPSS Versions 22 and 24 (IBM, Armonk, NY, USA). Intra- and inter-examiner reliability of the HU and noise measurements were analyzed by calculating the intraclass correlation coefficient. Bland–Altman plots comparing the examiners' readings were also obtained, and linear regression was used to test for proportional bias between the examiners' measurements. The Kolmogorov–Smirnov and Shapiro–Wilk tests of normality were performed for the subgroups imaged with a standard kernel, and indicated normal

distribution of the data in these groups. Therefore, paired *t* tests were used to compare the HU and noise measurements recorded from each of the test combinations of protocols with those from the reference dose/FBP technique protocol. Two-way ANOVA with repeated measures was used to analyze the effect of dose and reconstruction technique on the measurements. Level of significance was set at $p = 0.05$.

Results

Intra- and inter-examiner reliability of the mean HU were 0.996 and 0.987, respectively ($p < 0.001$). For the noise measurements, they were 0.991 and 0.974, respectively ($p < 0.001$). Bland–Altman plots with linear regression (see [electronic Supplementary Material](#)) did not demonstrate systematic variation between the examiners' measurements for either HU or noise ($p > 0.5$).

Mean HU

A statistically significant difference in the mean HUs was found between the reference dose/FBP protocol and almost all the test combinations ($p \leq 0.021$), regardless of the kernel used. Using bone kernel exceptions were those protocols using the reference dose with ASIR 50 ($p = 0.533$), ASIR 100 ($p = 0.096$), and MBIR ($P = 0.840$; Table 2). MBIR was only possible with standard kernel, but was compared with the reference dose/FBP protocol bone kernel as well. Using the standard kernel, exceptions were the reference dose with ASIR 100 ($p = 0.836$) and low-dose protocol 1 with MBIR ($p = 0.403$; see Table 3). Overall, the maximum mean differences in HU were 178.35 HU using the bone kernel and 273.74 HU using the standard kernel.

When a bone kernel was used (except with MBIR), there was a significant effect for the interaction between the dose and reconstruction techniques on the mean of the HU ($p = 0.007$). When the dose and reconstruction technique were considered separately, there was a significant difference in mean HU between the different dose protocols ($p < 0.001$) with an overall pattern of increase in HU with decreasing dose, except at the lowest-dose protocols. No significant difference in mean HU was found between the reconstruction techniques ($p = 0.353$).

However, when a standard kernel was used with all reconstruction techniques, there was no significant effect for the interaction between the dose and reconstruction techniques on the mean of the HU ($p = 0.318$), although there was a significant difference in mean HU between the different dose protocols ($p < 0.001$) and between the reconstruction techniques ($p < 0.001$). Interestingly, using the standard kernel, use of MBIR decreased the mean HU when compared with the corresponding FBP and

Table 2 Images of a sample site obtained using a bone kernel (except with MBIR) with the various combinations of dose protocols and reconstructions techniques. Mean HU and mean SD values (noise) at

region of interest (marked by square) for each dataset are noted above the image. All images were compared to the reference dose protocol with filtered backprojection (red frame). n.s.: no significant difference ($p = 0.05$)

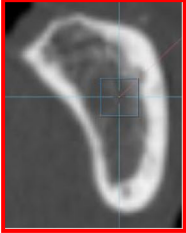
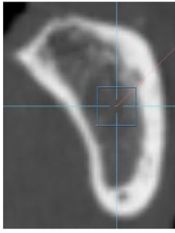
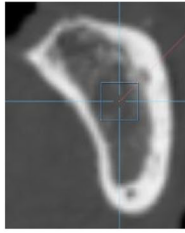
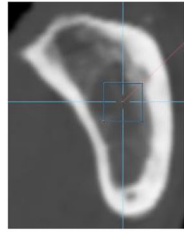
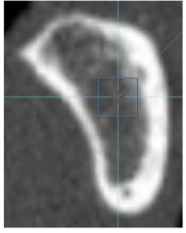
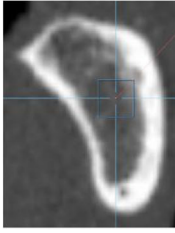
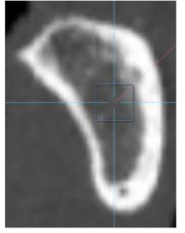
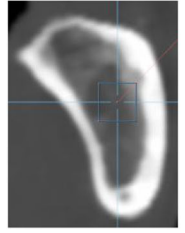
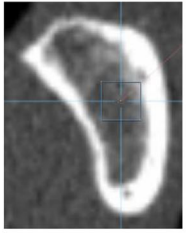
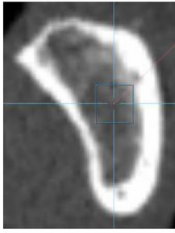
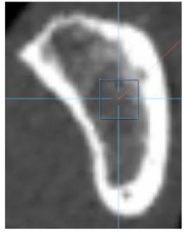
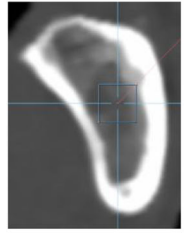
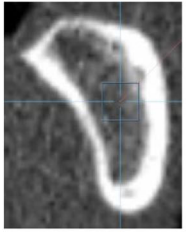
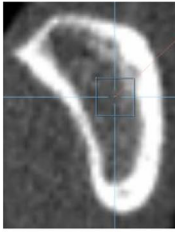
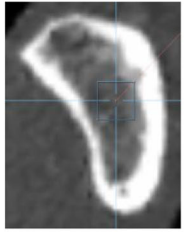
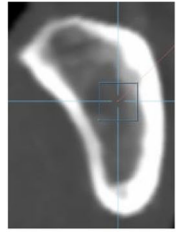
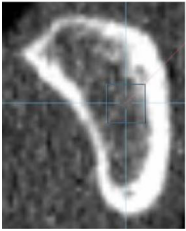
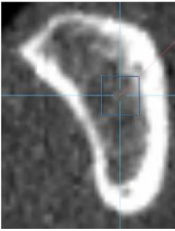
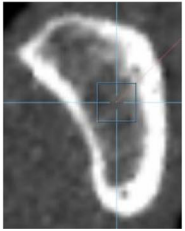
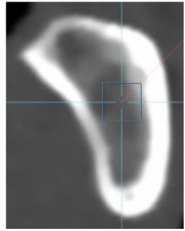
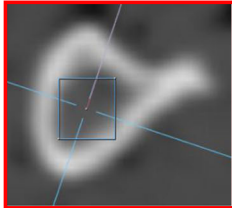
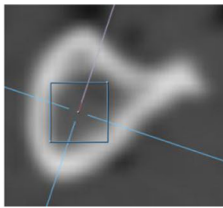
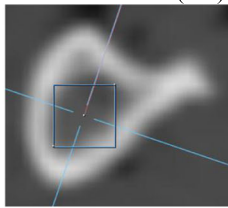
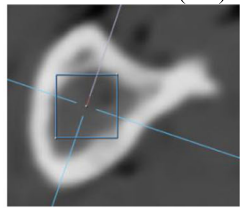
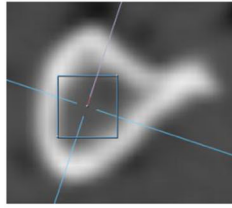
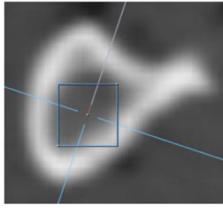
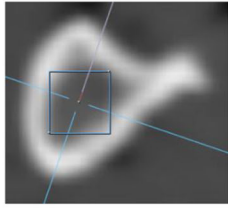
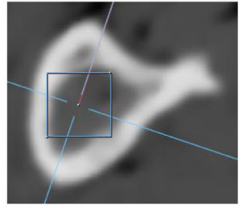
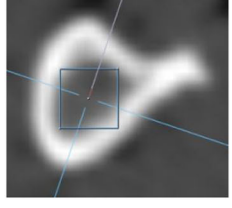
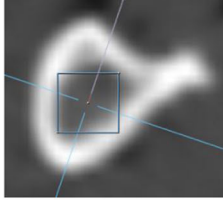
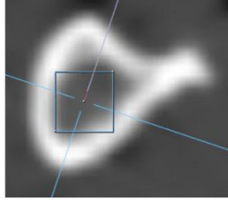
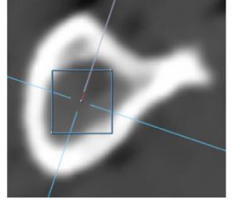
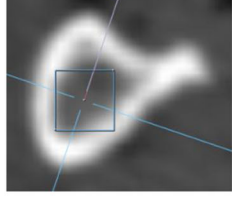
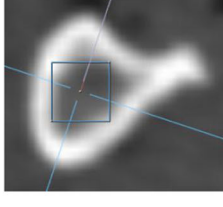
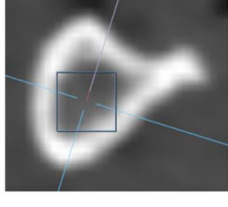
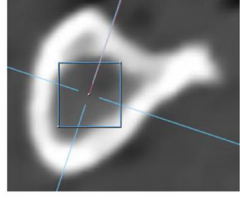
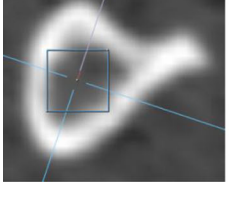
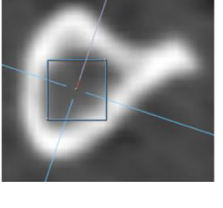
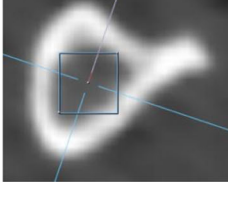
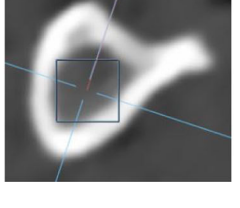
	Filtered Backprojection	ASIR 50	ASIR 100	MBIR
Reference dose protocol	Mean HU: 334.24 Mean SD: 308.37 	Mean HU: 342.28 (n.s.) Mean SD: 331.86 (n.s.) 	Mean HU: 298.22 (n.s.) Mean SD: 378.16 (n.s.) 	Mean HU: 336.40 (n.s.) Mean SD: 320.23 (n.s.) 
Low dose protocol 1	Mean HU: 394.66 Mean SD: 364.76 	Mean HU: 409.38 Mean SD: 374.74 	Mean HU: 407.53 Mean SD: 378.84 	Mean HU: 385.66 Mean SD: 334.97 
Low dose protocol 2	Mean HU: 464.87 Mean SD: 413.15 	Mean HU: 480.08 Mean SD: 429.30 	Mean HU: 462.71 Mean SD: 402.79 	Mean HU: 492.34 Mean SD: 414.25 
Low dose protocol 3	Mean HU: 478.56 Mean SD: 463.40 	Mean HU: 444.28 Mean SD: 416.50 	Mean HU: 512.59 Mean SD: 464.30 	Mean HU: 508.51 Mean SD: 403.13 
Low dose protocol 4	Mean HU: 489.52 Mean SD: 552.10 	Mean HU: 439.45 Mean SD: 469.03 	Mean HU: 428.65 Mean SD: 419.83 	Mean HU: 439.14 Mean SD: 344.66 

Table 3 Images of a sample site obtained using a standard kernel with the various combinations of exposure protocols and reconstructions techniques. Mean HU and mean SD values (noise) at region of interest

(marked by square) for each dataset are noted above the image. All images were compared to the reference dose protocol with filtered backprojection (red frame). n.s.: no significant difference ($p = 0.05$)

	Filtered Backprojection	ASIR 50	ASIR 100	MBIR
Reference dose protocol	Mean HU: 400.16 Mean SD: 349.74 	Mean HU: 428.48 Mean SD: 377.16 	Mean HU: 397.45 (n.s.) Mean SD: 344.72 (n.s.) 	Mean HU: 348.75 Mean SD: 383.02 (n.s.) 
Low dose protocol 1	Mean HU: 499.58 Mean SD: 428.94 	Mean HU: 458.31 Mean SD: 394.66 	Mean HU: 460.41 Mean SD: 400.44 	Mean HU: 384.28 (n.s.) Mean SD: 405.26 
Low dose protocol 2	Mean HU: 531.96 Mean SD: 442.79 	Mean HU: 544.68 Mean SD: 462.59 	Mean HU: 551.57 Mean SD: 463.91 	Mean HU: 478.44 Mean SD: 496.06 
Low dose protocol 3	Mean HU: 598.68 Mean SD: 503.62 	Mean HU: 587.57 Mean SD: 503.62 	Mean HU: 673.89 Mean SD: 447.99 	Mean HU: 473.66 Mean SD: 488.24 
Low dose protocol 4	Mean HU: 562.63 Mean SD: 487.84 	Mean HU: 571.49 Mean SD: 458.36 	Mean HU: 555.26 Mean SD: 467.71 	Mean HU: 469.59 Mean SD: 452.84 

ASIR images. The maximum difference of the mean HU obtained from the reference dose/FBP protocol and the

corresponding low-dose IV protocol was 162.48 HU using FBP but only 69.43 HU using MBIR.

Noise

A statistically significant difference in noise measurement (mean SD of HU measurements in bone) was found between the reference dose/FBP protocol and almost all the test combinations ($p \leq 0.033$). Using bone kernel exceptions were those protocols using the reference dose with ASIR 50 ($p = 0.053$), ASIR 100 ($p = 0.400$), and MBIR ($P = 0.300$; see Table 2). Using a standard kernel, exceptions were the reference dose with ASIR 100 ($p = 0.705$) and MBIR ($p = 0.111$; see Table 3). Overall, the maximum mean differences in noise were 243.73 using a bone kernel and 153.88 using a standard kernel.

There was a significant effect for the interaction between the dose and reconstruction techniques on the noise measurements when either a bone or standard kernel was used ($p = 0.037$ and 0.014 , respectively). When the dose and reconstruction techniques were considered separately, there was a significant difference in noise between the dose protocols when either a bone or standard kernel was used ($p < 0.001$), with progressively increasing noise as the dose decreased. However, there was no significant difference in noise levels between the lowest dose protocols.

When a bone kernel was used there was also a significant difference in noise between the reconstruction techniques ($p = 0.006$), with FBP and MBIR showing the highest and lowest noise levels, respectively, and no difference was found between ASIR 50 and ASIR 100. When a standard kernel was used there was no significant difference in noise between the reconstruction techniques ($p = 0.197$).

Discussion

The present study aimed to investigate the effect of using ultra-low doses in combination with various reconstruction techniques on the objective density and noise measurements of MDCT images of dental implant sites. The investigated protocols allowed for dose savings of about 89–98 % as compared with a current reference dose protocol for implant planning and guided surgery. Reduction of radiation exposure to ALARA “as low as reasonably achievable” levels is a major task in radiology, driven by both legislative authorities and medical societies. And although CBCT is becoming more widely utilized for implant site analysis, ultra-low-dose MDCT may have an advantage over CBCT for analysis of multiple implant sites and if the CT examination is to be used for CT-guided production of surgical guides.

The lowest-dose protocols applied in the present study utilized the lowest mA and kVp possible with the MDCT device used. The calculated effective doses ranged from 100–500 microSv. However, the scans included the entire head and mandible; so, limiting the field of view (FOV) to one jaw only

is expected to substantially lower the effective doses. Homolka et al. [28] showed that low-dose MDCT examination of the maxilla may impart an effective dose of 22 microSv, while that of a mandible may impart 123 microSv, which is comparable to a full-mouth survey with intra-oral films (150 microSv). Similar results were published by Cordasco et al. [16] who calculated mean absorbed dose using an ultra-low-dose MDCT protocol of $CTDI_{vol}$ of 2.5 mGy (comparable to the dose imparted by low-dose protocol 2 in the present study), which is similar to that related to conventional radiographic exams (lateral cephalogram + posterior-anterior cephalogram + panoramic), with a difference of about 0.06 mGy.

In order to standardize the area of interest and confine it to implant sites only, the size of the ROI selected was the largest possible size which would fit within the bone boundaries of all the sample sites. The largest possible ROI size was used in order to improve reproducibility of the measurements. The very high intra- and inter-examiner reliability obtained with the present technique indicates that positioning of the ROI was reproducible. Registration-based analysis is an alternative method which may also be used to ensure reproducible placement of the ROI.

The findings of the present study indicate that there was a significant difference in mean HU and noise between most of the test protocols and the reference dose/FBP protocol. The increase in mean HU with decreasing doses is expected considering the known effect of exposure parameters on the HU scale [24]. The lack of a significantly increasing mean HU observed between the lowest dose protocols in the present study may be due to the fact that the kVp, which is known to have an effect on the HU scale [29], was constant at the lowest-dose protocols. In dentomaxillofacial radiology where images are usually reconstructed using bone kernels, which are known to show higher accuracy compared to standard kernel for linear measurements of the jaws [30], additional reconstruction using a standard kernel and MBIR may potentially reduce HU variability for bone density evaluation in low-dose images.

The significant effect of the interaction between the dose and reconstruction techniques on mean HU found in the present study is in agreement with the findings of Herin et al. (2015) who reported higher HUs with a 70 % reduction in dose in combination with MBIR or ASIR 50 [31]. Furthermore, the lack of a significant difference in HU between reconstruction techniques when a bone kernel was used is in agreement with the findings of previous studies which found no difference in HU values of coronary artery plaque [32] or within the lungs [33] when FBP, ASIR, or MBIR were used. However, the significantly lower mean HU obtained with MBIR and standard kernel, compared to ASIR, in the present study is in contrast to the findings of Botsikas et al. (2014) who reported

significantly higher HU numbers for urinary tract stones with MBIR, compared to ASIR [34].

In general, standard kernels show less noise than bone kernels [35]. Interestingly, in the present study, the reconstruction technique had no significant effect on noise levels when a standard kernel was used and with bone kernel a significant difference in noise between ASIR 50 and ASIR 100 was not observed. These findings are in contrast with the findings of previous studies which reported that increasing the percentage of ASIR led to a decrease in image noise [33, 36], and that MBIR images demonstrated less noise than ASIR [34, 37, 38]. The differences may possibly be explained by the fact that the noise measurements in the present study were confined to bone, whereas the previous studies evaluated noise as standard deviation of HU measures in soft tissue such as the posterior fossa, lung, or fat, or within air, such as the maxillary sinus. Similar to the results of the present study, Schulz et al. showed that the effect of IRT on noise reduction is more pronounced with bone (hard) kernels compared to soft (standard) kernels [37].

The clinical significance of the variations in HU and noise on implant treatment planning and surgery is still not clear. Standard-dose FBP protocols have been found to provide accurate 3D models of the jaws [10–13]. Furthermore, ultra-low-dose protocols combined with IRT, utilizing dose reductions of more than 90 % compared to standard protocols, did not significantly interfere with subjective image quality of 3D models [38]. The accuracy of thresholding with these protocols is relevant to the CAD/CAM production of surgical stents for dental implant surgery; so, the effect of increased density and noise on thresholding accuracy needs to be investigated for the various combinations of ultra-low-dose protocols. Other implant imaging tasks which may possibly be affected by image noise are identification of anatomic margins and trabecular bone changes. Relevant studies performed with the various dose/reconstruction technique combinations may include evaluation of contrast noise ratios and morphometric analysis [39, 40].

The impact of the observed differences in noise and density between the various protocols on objective bone quality evaluation during implant site analysis is also still not clear. For previous investigators have related HU to bone density using HU values acquired with standard dose protocols and FBP. Although a wide range of HUs may be seen within each of the bone quality types described by Lekholm and Zarb (1985) [41], Norton and Gamble (2001) [42] published quantitative ranges for these bone quality types. Type 1 bone had an HU greater than +850. Type 2 and Type 3 bone were found to have overlapping HUs, mostly ranging from +500 to +800 HU. Type 4 bone had an HU range of less than 0 to +500.

An important aim of the present study was to demonstrate whether HU measurements remain stable with the

currently available ultra-low-dose technology and IRTs. Different dose/reconstruction protocols were found to have different effects on HU. Although the observed maximum mean differences in HU of 178.35 (bone kernel) and 273.74 (standard kernel) obtained with low-dose protocols (compared with the standard protocol) may provide a false classification of bone quality, MBIR showed a lower discrepancy in HUs with ultra-low doses than the other reconstruction techniques. The difference of the mean HU obtained from the reference dose/FBP protocol and the low-dose protocol IV was 162.48 HU using FBP but only 69.43 HU using MBIR. Clinicians should be aware that MBIR may provide lower variability in HUs than other reconstruction techniques, but that HU values are not absolute values.

Furthermore, although modification of implant treatment planning on the basis of bone density has been advocated by some authors [43, 44], and primary implant stability has been correlated with bone density measurements recorded from MDCT [3–6], the effect of the combinations of the ultra-low doses and various reconstruction techniques on the determinants of implant stability still needs to be investigated. There is still no reference standard relating MDCT HU values to any of the determinants of implant site treatment planning and/or success [45]. In order to develop reference standards, reliable density values must be correlated with the various measures of implant stability and/or success for each combination of MDCT dose/reconstruction technique [46].

Acknowledgments The authors wish to thank individuals who donated their bodies and tissues for the advancement of education and research. The scientific guarantor of this publication is Dr. Gerlig Widmann. The authors of this manuscript declare no relationships with any companies whose products or services may be related to the subject matter of the article. The authors state that this work has not received any funding. Amal Ahmed Gaber Abd-Alhafez, MSc (private consultant) and Eidah Alenazi, MSc (Assistant Researcher, Statistics & Operations Research Department, Kind Saud University) kindly provided statistical advice for this manuscript. Institutional review board approval was not required because the bodies used in the study were donated by people who had given their informed consent for their use for scientific and educational purposes prior to death and the study fulfilled all requirements necessary for studies on human cadavers according to the regulations of the Division of Clinical and Functional Anatomy, Medical University of Innsbruck. Written informed consent was obtained from all subjects (patients) in this study. Some study subjects or cohorts have been previously reported in the following experimental studies: *Widmann G. et al., Ultralow-dose computed tomography imaging for surgery of midfacial and orbital fractures using ASIR and MBIR. International Journal of Oral and Maxillofacial Surgery. 2015. 44(4): p. 441–446*, and *Widmann, G. et al., Ultralow-Dose CT of the Craniofacial Bone for Navigated Surgery Using Adaptive Statistical Iterative Reconstruction and Model-Based Iterative Reconstruction: 2D and 3D Image Quality. American Journal of Roentgenology, 2015. 204(3): p. 563–569*. Methodology: retrospective, experimental, multicenter study.

References

- Homer K (2013) Cone-beam computed tomography: time for an evidence-based approach. *Prim Dent J* 2:22–31
- Nackaerts O, Maes F, Yan H, Couto Souza P, Pauwels R, Jacobs R (2011) Analysis of intensity variability in multislice and cone beam computed tomography. *Clin Oral Implants Res* 22:873–879
- Turkylmaz I, McGlumphy EA (2008) Influence of bone density on implant stability parameters and implant success: a retrospective clinical study. *BMC Oral Health* 8:32
- Turkylmaz I, McGlumphy EA (2008) Is there a lower threshold value of bone density for early loading protocols of dental implants? *J Oral Rehabil* 35:775–781
- Ikumi N, Tsutsumi S (2005) Assessment of correlation between computerized tomography values of the bone and cutting torque values at implant placement: a clinical study. *Int J Oral Maxillofac Implants* 20:253–260
- Merheb J, Van Assche N, Coucke W, Jacobs R, Naert I, Quirynen M (2010) Relationship between cortical bone thickness or computerized tomography-derived bone density values and implant stability. *Clin Oral Implants Res* 21:612–617
- Aranyarachkul P, Caruso J, Gantes B et al (2005) Bone density assessments of dental implant sites: 2. Quantitative cone-beam computerized tomography. *Int J Oral Maxillofac Implants* 20:416–424
- Isoda K, Ayukawa Y, Tsukiyama Y, Sogo M, Matsushita Y, Koyano K (2012) Relationship between the bone density estimated by cone-beam computed tomography and the primary stability of dental implants. *Clin Oral Implants Res* 23:832–836
- Beer A, Gahleitner A, Holm A, Tschabitscher M, Homolka P (2003) Correlation of insertion torques with bone mineral density from dental quantitative CT in the mandible. *Clin Oral Implants Res* 14:616–620
- Liang X, Lambrichts I, Sun Y et al (2010) A comparative evaluation of cone beam computed tomography (CBCT) and multi-slice CT (MSCT). Part II: On 3D model accuracy. *Eur J Radiol* 75:270–274
- Primo B, Presotto A, de Oliveira H et al (2012) Accuracy assessment of prototypes produced using multi-slice and cone-beam computed tomography. *Int J Oral Maxillofac Surg* 41:1291–1295
- Loubele M, Maes F, Schutyser F, Marchal G, Jacobs R, Suetens P (2006) Assessment of bone segmentation quality of cone-beam CT versus multislice spiral CT: a pilot study. *Oral Surg Oral Med Oral Pathol Oral Radiol Endod* 102:225–234
- Mah P, Reeves TE, McDavid WD (2010) Deriving Hounsfield units using grey levels in cone beam computed tomography. *Dentomaxillofac Radiol* 39:323–335
- United Nations Scientific Committee on the Effects of Atomic Radiation (2008) Sources and effects of ionizing radiation. Official records of the general assembly, sixty-third session, supplement No 46. United Nations, New York
- Tyndall DA, Price JB, Tetradis S, Ganz SD, Hildebolt C, Scarfe WC (2012) Position statement of the American Academy of Oral and Maxillofacial Radiology on selection criteria for the use of radiology in dental implantology with emphasis on cone beam computed tomography. *Oral Surg Oral Med Oral Pathol Oral Radiol* 113:817–826
- Cordasco G, Portelli M, Militi A et al (2013) Low-dose protocol of the spiral CT in orthodontics: comparative evaluation of entrance skin dose with traditional X-ray techniques. *Prog Orthod* 14:24
- Jeong DK, Lee SC, Huh KH et al (2012) Comparison of effective dose for imaging of mandible between multi-detector CT and cone-beam CT. *Imaging Sci Dent* 42:65–70
- Widmann G, Dalla Torre D, Hoermann R et al (2015) Ultralow-dose computed tomography imaging for surgery of midfacial and orbital fractures using ASIR and MBIR. *Int J Oral Maxillofac Surg* 44:441–446
- Ludlow J, Timothy R, Walker C et al (2015) Effective dose of dental CBCT—a meta analysis of published data and additional data for nine CBCT units. *Dento Maxillo Facial Radiol* 44:20140197
- Kyriakou Y, Kolditz D, Langner O, Krause J, Kalender W (2011) Digital volume tomography (DVT) and multislice spiral CT (MSCT): an objective examination of dose and image quality. *Röfo* 183:144–153
- Bulla S, Blanke P, Hassepass F et al (2012) Reducing the radiation dose for low-dose CT of the paranasal sinuses using iterative reconstruction: feasibility and image quality. *Eur J Radiol* 81:2246–2250
- Silva AC, Lawder HJ, Hara A, Kujak J, Pavlicek W (2010) Innovations in CT dose reduction strategy: application of the adaptive statistical iterative reconstruction algorithm. *Am J Roentgenol* 194:191–199
- Molteni R (2013) Prospects and challenges of rendering tissue density in Hounsfield units for cone beam computed tomography. *Oral Surg Oral Med Oral Pathol Oral Radiol* 116:105–119
- NIST (National Institute of Science and technology) (Last updated: May 19, 2015) Tables of x-ray mass attenuation coefficients and mass energy-absorption coefficients from 1 keV to 20 MeV for elements Z = 1 to 92 and 48 additional substances of dosimetric interest*. Available via <http://www.nist.gov/pml/data/xraycoef/index.cfm> July 6th, 2015
- McHanwell S, Brenner E, Chirculescu A et al (2008) The legal and ethical framework governing Body Donation in Europe - A review of current practice and recommendations for good practice. *Eur J Anat* 12:1–24
- Riederer B, Bolt S, Brenner E et al (2012) The legal and ethical framework governing Body Donation in Europe - 1st update on current practice. *Eur J Anat* 16:1–21
- Platzer W, Putz R, Poisel S (1978) Ein neues Konservierungs- und Aufbewahrungssystem für anatomisches Material. *Acta Anat (Basel)* 102:60–67
- Homolka P, Gahleitner A, Kudler H, Nowotny R (2001) A simple method for estimating effective dose in dental CT. Conversion factors and calculation examples for a clinical low dose protocol. *RoFo: Fortschritte auf dem Gebiete der Rontgenstrahlen und der Nuklearmedizin* 173:558–562
- Todisco M, Trisi P (2005) Bone mineral density and bone histomorphometry are statistically related. *Int J Oral Maxillofac Implants* 20:898–904
- Loubele M, Van Assche N, Carpentier K et al (2008) Comparative localized linear accuracy of small-field cone-beam CT and multi-slice CT for alveolar bone measurements. *Oral Surg Oral Med Oral Pathol Oral Radiol Endod* 105:512–518
- Hérin E, Gardavaud F, Chiaradia M et al (2015) Use of Model-Based Iterative Reconstruction (MBIR) in reduced-dose CT for routine follow-up of patients with malignant lymphoma: dose savings, image quality and phantom study. *European radiology*:1–9
- Puchner SB, Ferencik M, Maurovich-Horvat P et al (2015) Iterative image reconstruction algorithms in coronary CT angiography improve the detection of lipid-core plaque—a comparison with histology. *Eur Radiol* 25:15–23
- Hague CJ, Krowchuk N, Alhassan D et al (2014) Qualitative and quantitative assessment of smoking-related lung disease: effect of iterative reconstruction on low-dose computed tomographic examinations. *J Thorac Imaging* 29:350–356
- Botsikas D, Stefanelli S, Boudabbous S, Toso S, Becker CD, Montet X (2014) Model-based iterative reconstruction versus adaptive statistical iterative reconstruction in low-dose abdominal CT for urolithiasis. *AJR Am J Roentgenol* 203:336–340
- Hoxworth JM, Lal D, Fletcher GP et al (2014) Radiation dose reduction in paranasal sinus CT using model-based iterative reconstruction. *AJNR Am J Neuroradiol* 35:644–649

36. Hara AK, Paden RG, Silva AC, Kujak JL, Lawder HJ, Pavlicek W (2009) Iterative reconstruction technique for reducing body radiation dose at CT: feasibility study. *Am J Roentgenol* 193:764–771
37. Schulz B, Beeres M, Bodelle B et al (2013) Performance of iterative image reconstruction in CT of the paranasal sinuses: a phantom study. *AJNR Am J Neuroradiol* 34:1072–1076
38. Widmann G, Schullian P, Gassner E-M, Hoermann R, Bale R, Puelacher W (2015) Ultralow-dose CT of the craniofacial bone for navigated surgery using adaptive statistical iterative reconstruction and model-based iterative reconstruction: 2D and 3D image quality. *Am J Roentgenol* 204:563–569
39. Pauwels R, Silkosessak O, Jacobs R, Bogaerts R, Bosmans H, Panmekiate S (2014) A pragmatic approach to determine the optimal kVp in cone beam CT: balancing contrast-to-noise ratio and radiation dose. *Dentomaxillofac Radiol* 43: 20140059
40. Van Dessel J, Huang Y, Depypere M, Rubira-Bullen I, Maes F, Jacobs R (2013) A comparative evaluation of cone beam CT and micro-CT on trabecular bone structures in the human mandible. *Dentomaxillofac Radiol* 42:20130145
41. Lekholm U (1985) Tissue-integrated prosthesis: osseointegration in clinical dentistry. Quintessence, Chicago, pp 199–209
42. Norton MR, Gamble C (2001) Bone classification: an objective scale of bone density using the computerized tomography scan. *Clin Oral Implants Res* 12:79–84
43. Misch CE (2008) Contemporary implant dentistry. Mosby Incorporated, St. Louis
44. Ericsson I, Nilner K (2002) Early functional loading using Brånemark dental implants. *Int J Periodontics Restorative Dent* 22:9
45. Al-Ekrish AA (2014) Bone quality for implants. In: Tamimi D (ed) Specialty imaging dental implants. Elsevier, Altona, pp 1/30–31/37
46. Homolka P, Beer A, Birkfellner W et al (2002) Bone mineral density measurement with dental quantitative CT prior to dental implant placement in cadaver mandibles: pilot study. *Radiology* 224: 247–252